Supporting Information

Directed self-assembly of microcomponents enabled by laser-activated bubble latching

Li Jiang and David Erickson

Bubble growth data

All bubble growth measurements are shown in Figure S1*a*. Red data points represent bubbles that were confined within the hubs and blue data points represent bubbles that were not confined. Figure S1*b* shows the averages of the bubble sizes taken from frames immediately before and immediately after the sudden expansion. We see that in both the confined and unconfined cases, the bubble first grows steadily to 50μm before the expansion. After the expansion, while the confined bubbles average at 100μm, the unconfined bubbles grow to about 150μm.

Force Experiments

Different tile design

For the force experiments a different tile design is used for two purposes, as shown in Figure S2. One, the second layer of the tile fills the entire square, as opposed to being only the rings that make up the hub as in the first design. This way, we can assume there is negligible flow under the tile as compared to above it, and therefore a Poiseuille flow profile can be adopted between the top of the tile and the channel. Second, each side of the tile houses three hubs, also 50μm in radius, so that force calculations can be easily done with multiple bubble latches. Dimensions of the tiles and the thickness of the layers were kept consistent between the two designs. Taking the density of SU-8 2025 as $1.22 g/cm^3$ and the dimensions of the tile to be 500µm × 500µm × 30µm, we find the gravitational force to be 18.3µN and the buoyancy force to be 15µN, resulting in a net downward force of 3.3µN.

Problems with sticking between SU-8 and PDMS

During initial experiments, we observed that through generating a bubble on the SU-8, the heated tile often came into contact with the PDMS wall. The PDMS was subsequently heated, as shown by bubbles created inside the wall (Figure S3). The heating of the two materials while in contact caused the SU-8 tile to become stuck to the PDMS such that the tile would not move even at high flow rates. For the bending and reconfiguration experiments, this issue was avoided by flipping the microfluidic device upside down after the tiles are inserted so that the heated region of the tile never comes in contact with the PDMS. For force measurement experiments, the chips were also flipped upside down to maintain the same procedure throughout. However, now we are able to selectively secure one tile to the channel wall while allowing another to be dragged by the flow, giving sensible values for the flow rates at which the bubble links break.

Supplementary Figures

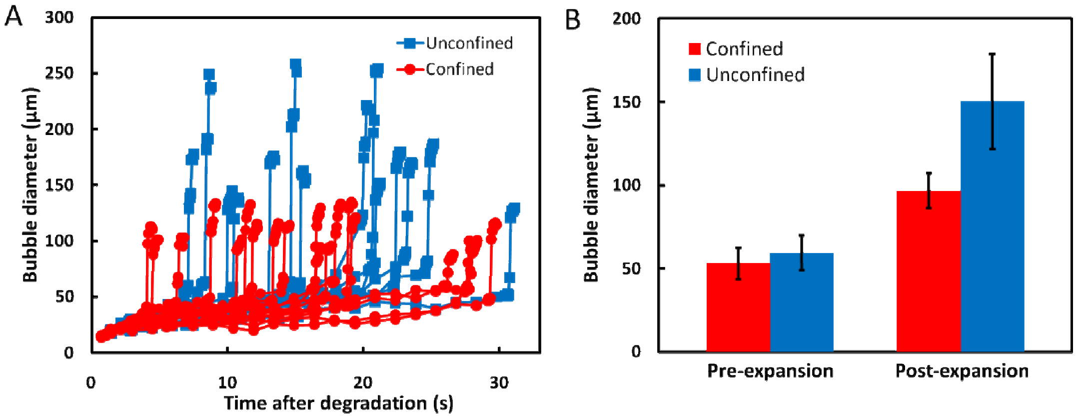

Supplementary Figure S1. Growth data of confined and unconfined bubbles. (a) Plot of 34 total measurements of the bubble size. (b) The average diameter of the bubble immediately before and after the expansion for both confined and unconfined cases. Before the expansion, both cases reach about 50µm, while after the expansion, the unconfined bubbles grow much larger than confined ones. Error bars represent one standard deviation.

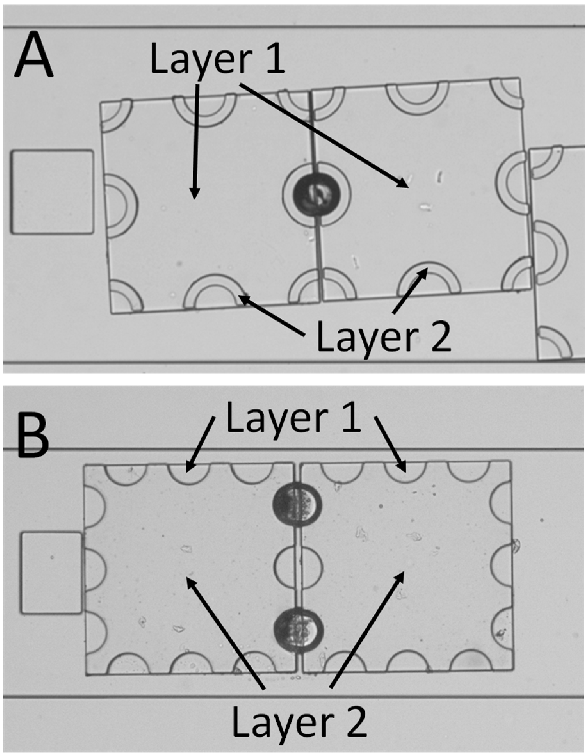

Supplementary Figure S2. Tiles used for demonstrations and force measurements. (a) Tiles used for bubble growth experiments and all demonstrations. The second layer of SU-8 makes up only the rings. (b) Tiles used for force measurements. The second layer fills the entire square except for the hub locations.

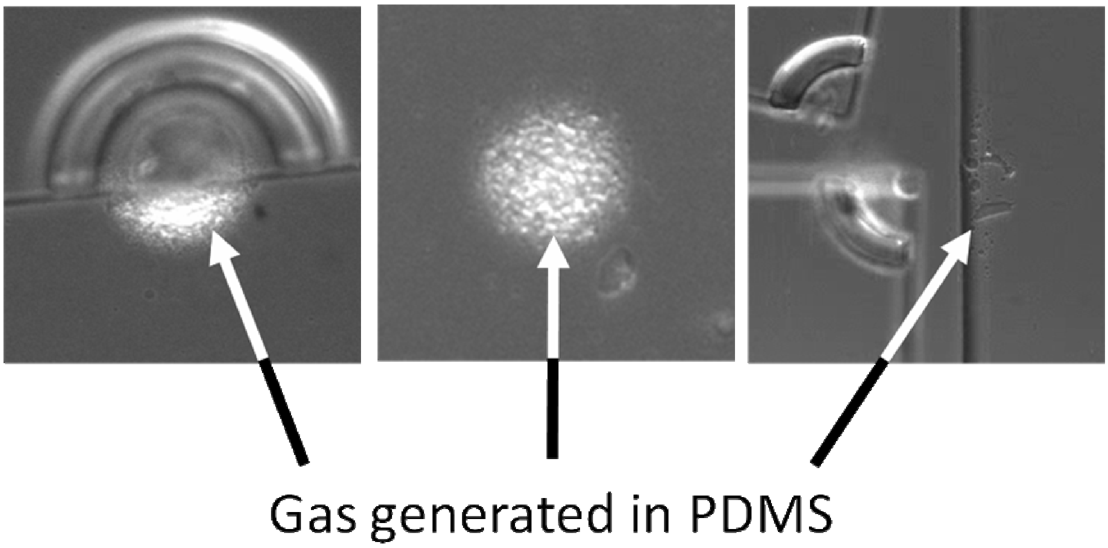

Supplementary Figure S3. Heat from SU-8 creates what appears to be bubbles in PDMS. If the laser is kept on for long enough, the tile becomes stuck on the PDMS wall.

Movie Legend

Movie 1. Connecting components through laser-activated bubble latching. Two initially misaligned tiles are linked and aligned by a bubble created through laser heating. Tile docking is also shown, in which the bubble is produced on only one tile. A second tile is then brought into contact with the bubble. The two tiles are linked and transported together.

Movie 2. Complex structures created via "controlled disassembly" using bubble latching. We create a hanging structure, where the inner tiles are removed after producing bubbles to latch the outer tiles. Next, we show the assembly of multiple structures in parallel. Lastly, we demonstrate multi-step assembly to create voids in structures.

Movie 3. Rigid/flexible transition of an assembled structure. First, four tiles are loosely connected and misaligned. By decreasing the pressure in the chamber, the bubbles are compressed, realigning the structure. Second, rigidly connected tiles are unable to pass a corner. Decreasing the pressure in the channel expands the bubbles, which transitions the structure to become flexible, allowing it to bend around the corner. Afterwards, pressure is increased to realign the tiles.

Movie 4. Bubble hinge reconfiguration demonstrations. Beginning with the "I" shape, we demonstrate reconfiguration into subsequent "L," "O," "T," and "Z," shapes. We also show a failed "L" to "T" reconfiguration attempt when a bubble hinge is not used. Finally, we show the motion of a latched "O" structure compared to an "O" shape that is not latched, in which case the tiles spread away from each other.